

SYSTEMS AND METHODS FOR DETERMINING BLOOD  
OXYGEN SATURATION VALUES USING COMPLEX NUMBER  
ENCODING

Mohamed K. Diab

Appl. No.: Unknown Atty Docket: MLABS.021A

1 / 24

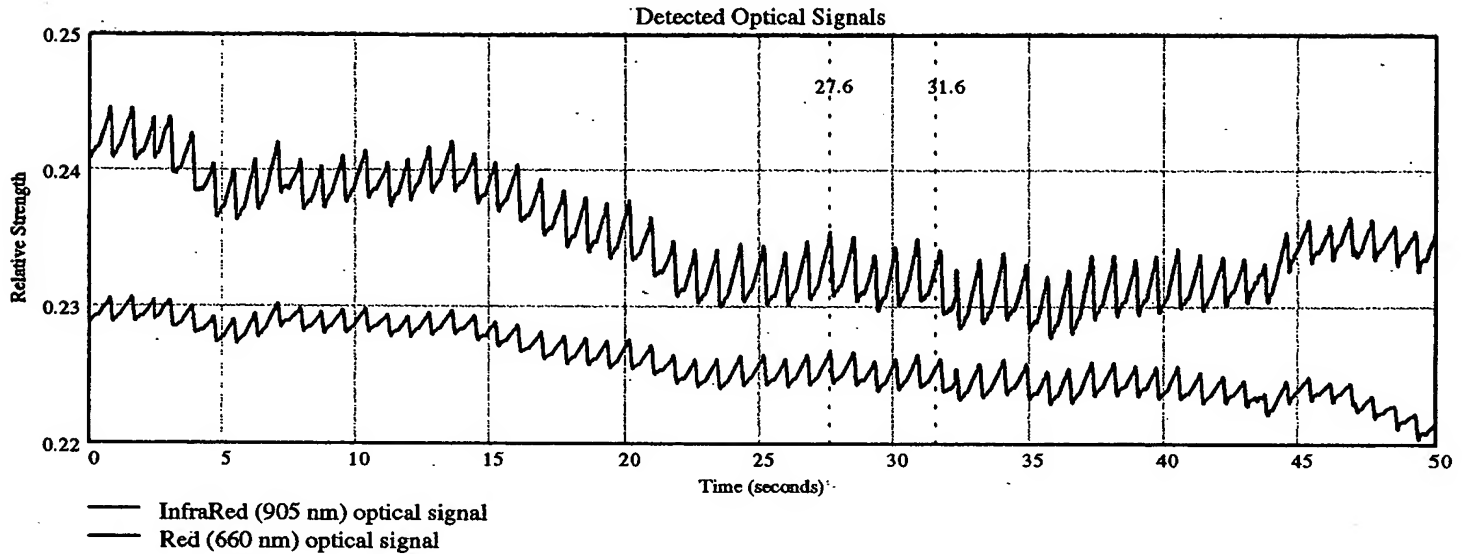


Figure 1. Detected optical signals from an adult male over a 50 seconds time interval. Markers indicate section from which subsequent photopleths were extracted and filtered.

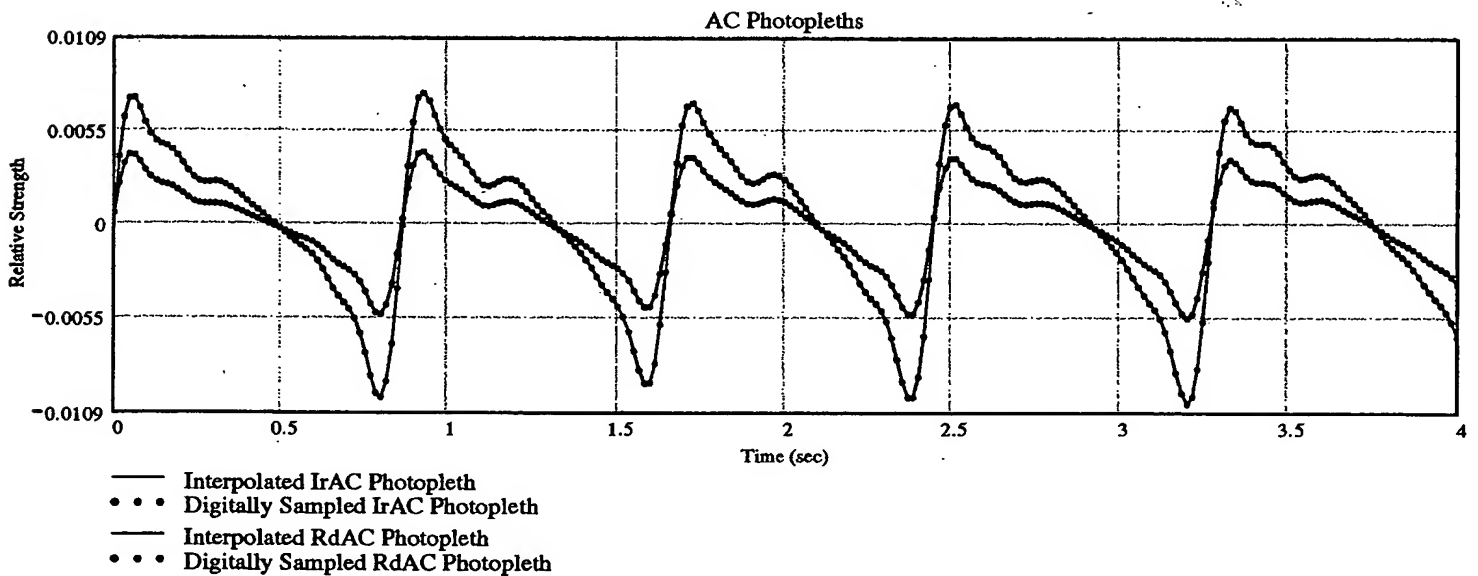


Fig. 2. Normalized and Bandpassed Red and InfraRed photopleths vs.time. Digital sampling rate is 62.5 Hz.

SYSTEMS AND METHODS FOR DETERMINING BLOOD  
OXYGEN SATURATION VALUES USING COMPLEX NUMBER  
ENCODING

Mohamed K. Diab

Appl. No.: Unknown Atty Docket: MLABS.021A

2 / 24

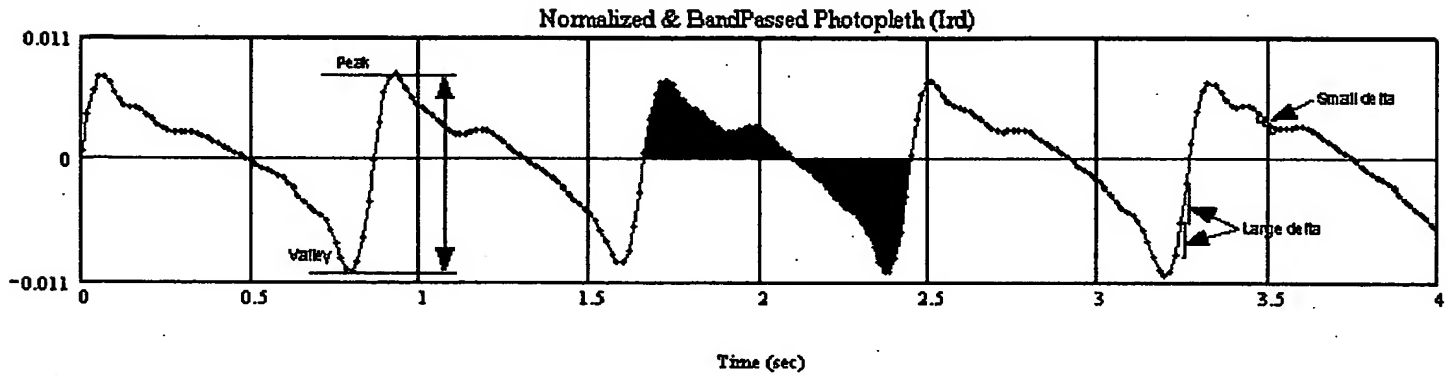


Figure 3. Previous techniques for calculating the strength of a photopleth. Peak-to-valley, area and differential technique (Biox pulse oximeter.)

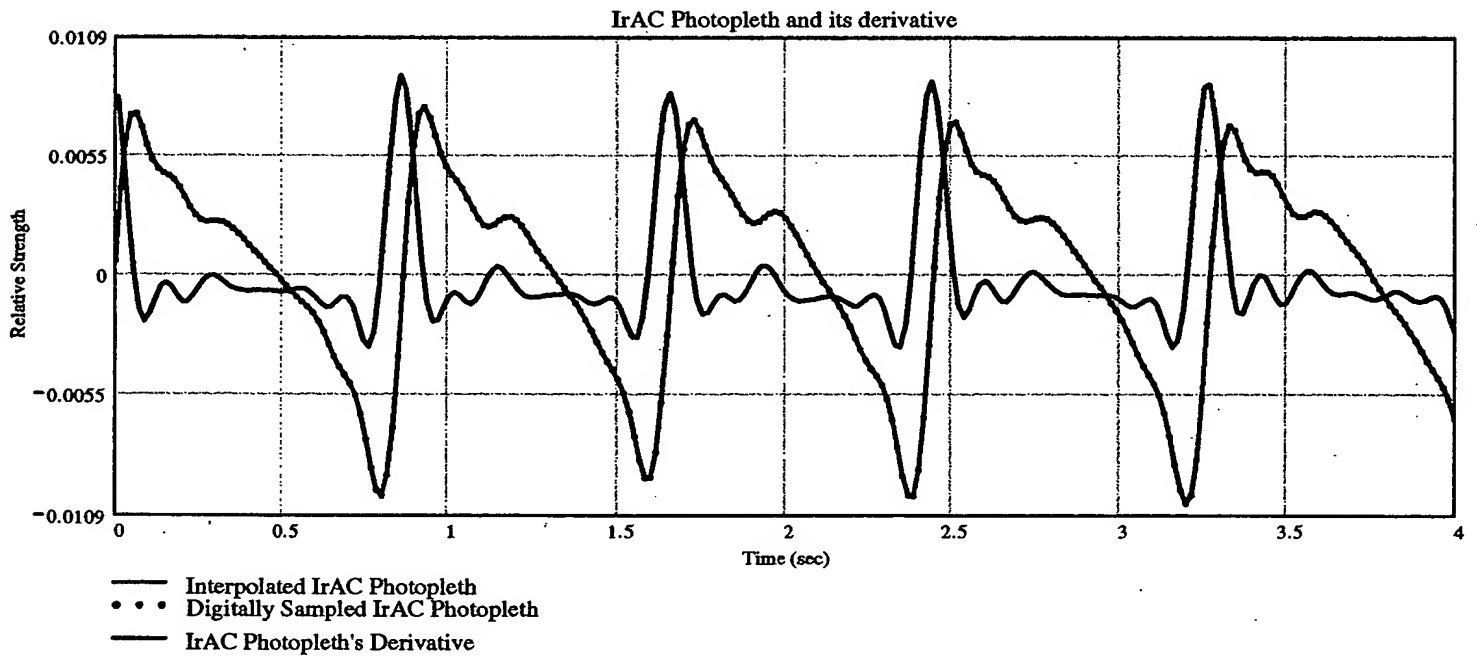


Fig 4. IrAC photopleth and its derivative vs. time

SYSTEMS AND METHODS FOR DETERMINING BLOOD  
OXYGEN SATURATION VALUES USING COMPLEX NUMBER  
ENCODING

Mohamed K. Diab

Appl. No.: Unknown Atty Docket: MLABS.021A

3/24

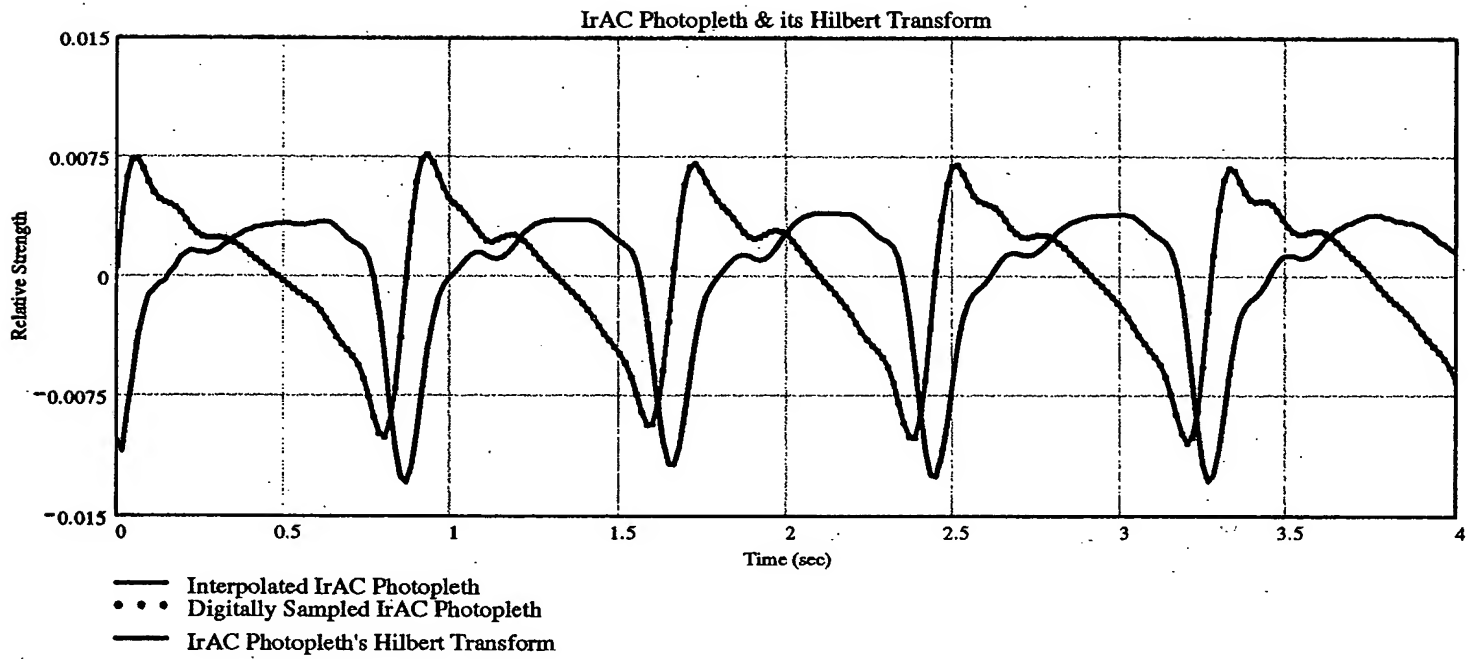


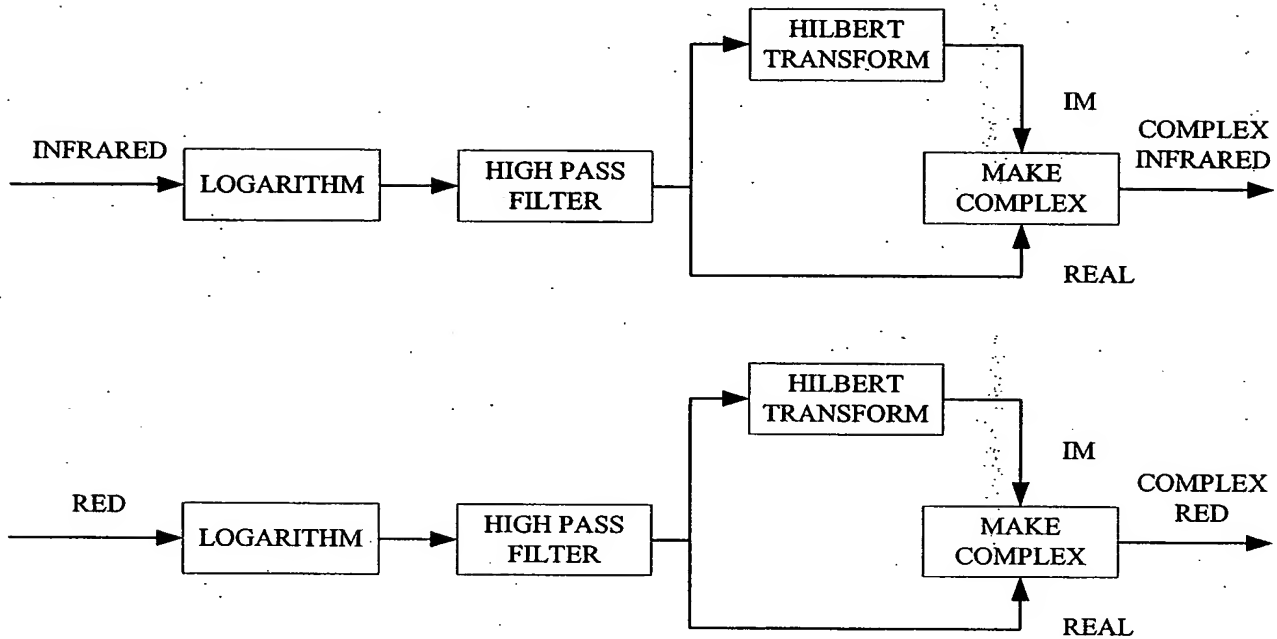
Fig 4A. IrAC photopleth and its Hilbert Transform vs. time

SYSTEMS AND METHODS FOR DETERMINING BLOOD  
OXYGEN SATURATION VALUES USING COMPLEX NUMBER  
ENCODING

Mohamed K. Diab

Appl. No.: Unknown Atty Docket: MLABS.021A

4 / 24



TYPE A, 0 PHASE SHIFT

Figure 5. Block diagram to generate type A complex photopleth waveforms

SYSTEMS AND METHODS FOR DETERMINING BLOOD  
OXYGEN SATURATION VALUES USING COMPLEX NUMBER  
ENCODING

Mohamed K. Diab

Appl. No.: Unknown Atty Docket: MLABS.021A

5/24

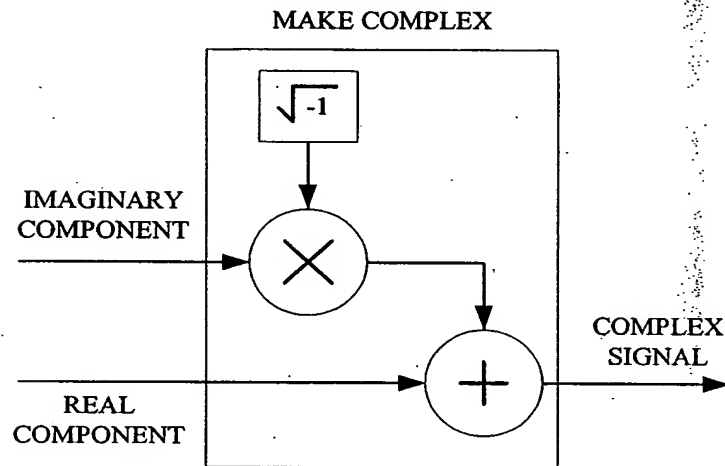


Figure 5A. Block diagram to make complex signals

SYSTEMS AND METHODS FOR DETERMINING BLOOD  
OXYGEN SATURATION VALUES USING COMPLEX NUMBER  
ENCODING

Mohamed K. Diab

Appl. No.: Unknown Atty Docket: MLABS.021A

6/24

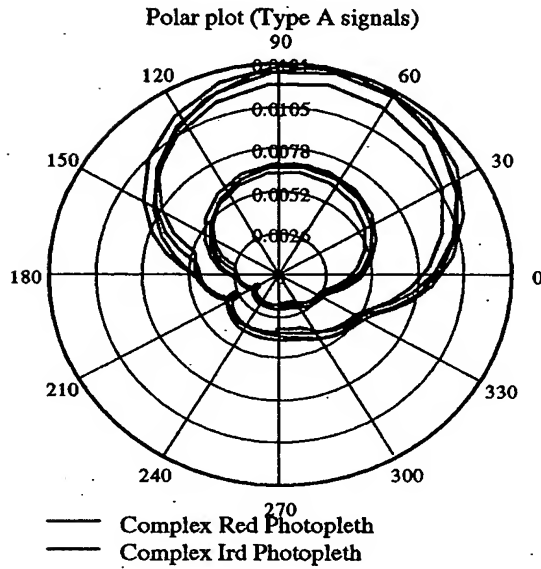


Figure 6. Polar plot of type A complex photopleths

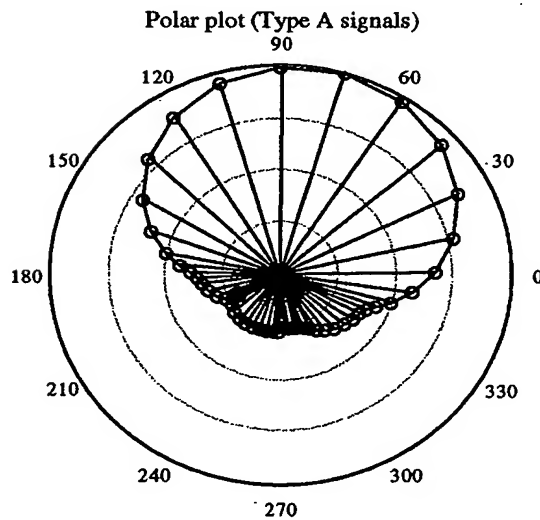
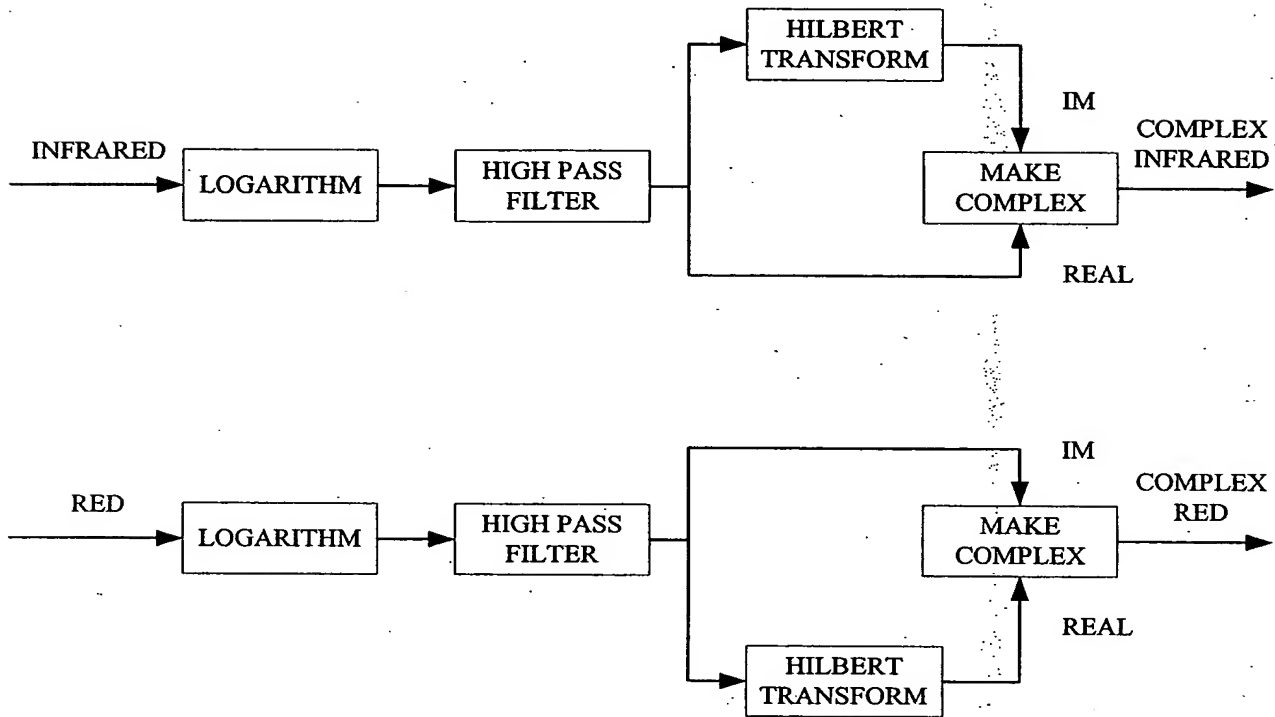


Figure 7. Area calculation for type A complex photopleth

SYSTEMS AND METHODS FOR DETERMINING BLOOD  
OXYGEN SATURATION VALUES USING COMPLEX NUMBER  
ENCODING

Mohamed K. Diab

Appl. No.: Unknown Atty Docket: MLABS.021A  
7/24



TYPE B,  $\frac{\pi}{2}$  PHASE SHIFT

Figure 8. Block diagram to generate type B complex photopleth waveforms

SYSTEMS AND METHODS FOR DETERMINING BLOOD  
OXYGEN SATURATION VALUES USING COMPLEX NUMBER  
ENCODING

Mohamed K. Diab

Appl. No.: Unknown Atty Docket: MLABS.021A  
8 / 24

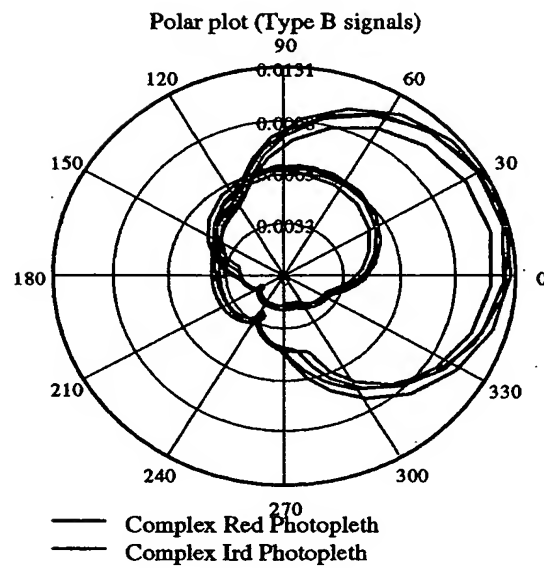


Figure 9. Polar plot of type B complex photopleths

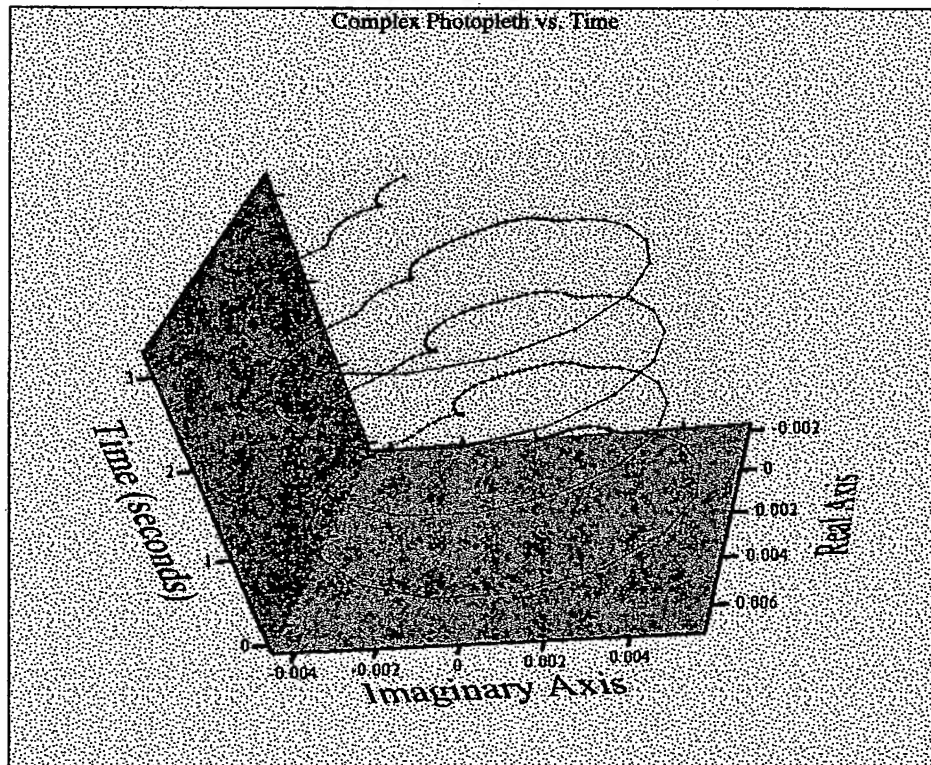


SYSTEMS AND METHODS FOR DETERMINING BLOOD  
OXYGEN SATURATION VALUES USING COMPLEX NUMBER  
ENCODING

Mohamed K. Diab

Appl. No.: Unknown Atty Docket: MLABS.021A

9 / 24



C

Fig. 10. 3D plot of type B complex photopleth vs. time

SYSTEMS AND METHODS FOR DETERMINING BLOOD  
OXYGEN SATURATION VALUES USING COMPLEX NUMBER  
ENCODING

Mohamed K. Diab

Appl. No.: Unknown Atty Docket: MLABS.021A  
10/24

Generation of Complex Ratios

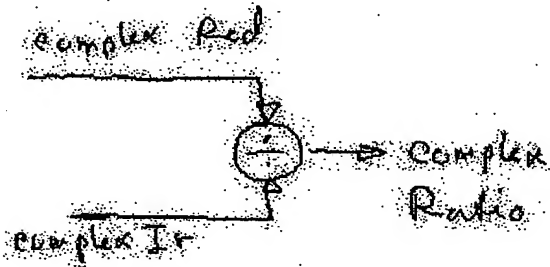


Figure 11. Block diagram for generating complex ratios

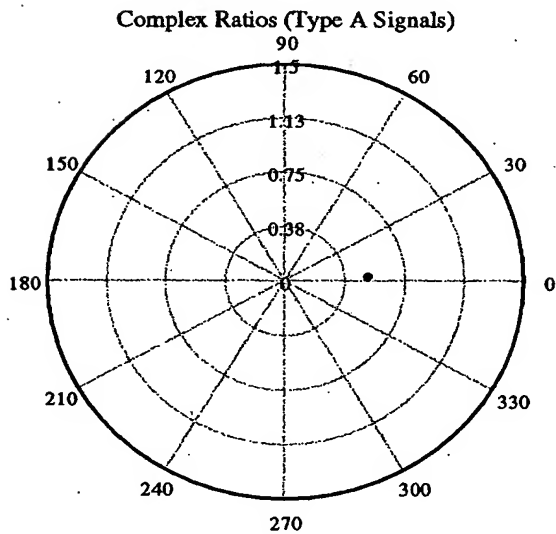


Figure 12. Complex ratios, steady saturation, for type A signals

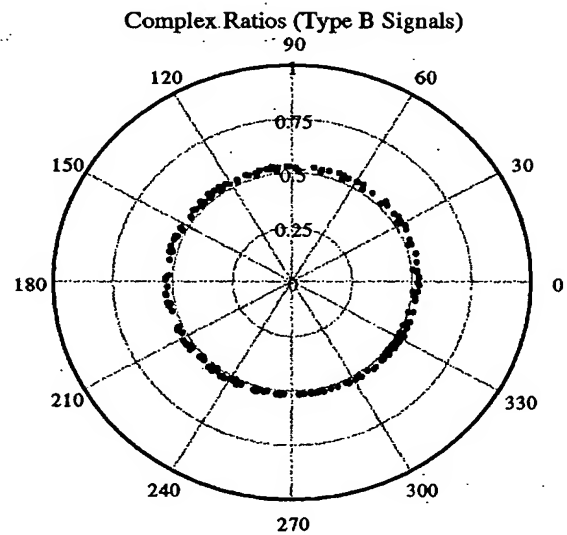
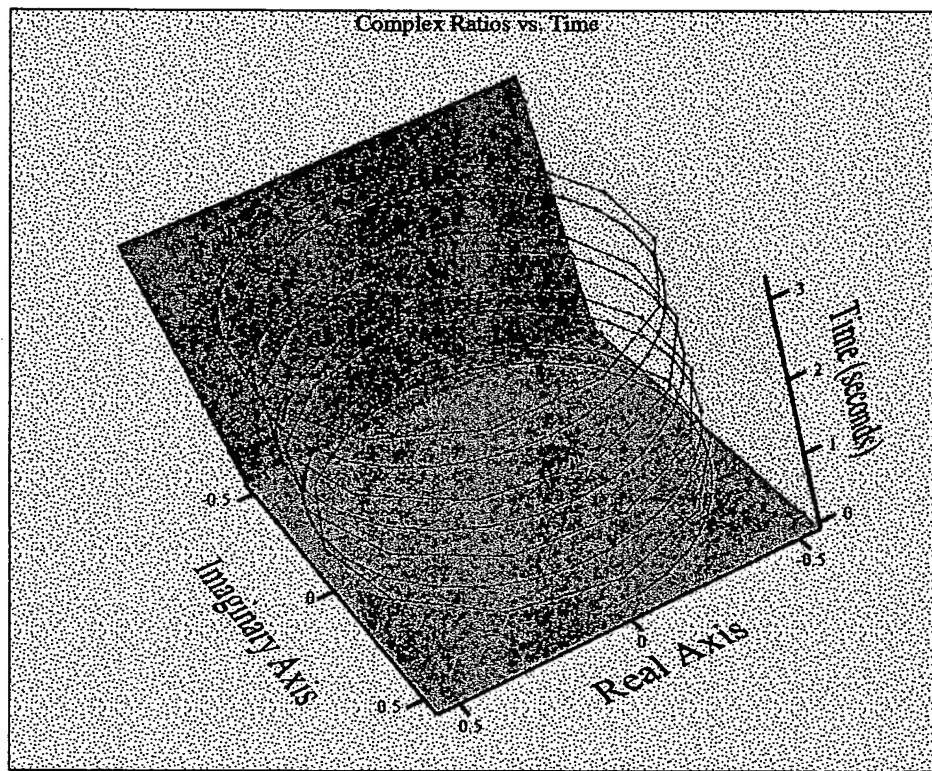


Figure 13. Complex ratios, steady saturation, for type B signals

SYSTEMS AND METHODS FOR DETERMINING BLOOD  
OXYGEN SATURATION VALUES USING COMPLEX NUMBER  
ENCODING

Mohamed K. Diab

Appl. No.: Unknown      Atty Docket: MLABS.021A  
11/24



C

Figure 14. 3D plot of Complex ratios vs. time

SYSTEMS AND METHODS FOR DETERMINING BLOOD  
OXYGEN SATURATION VALUES USING COMPLEX NUMBER  
ENCODING

Mohamed K. Diab

Appl. No.: Unknown Atty Docket: MLABS.021A

12 / 24

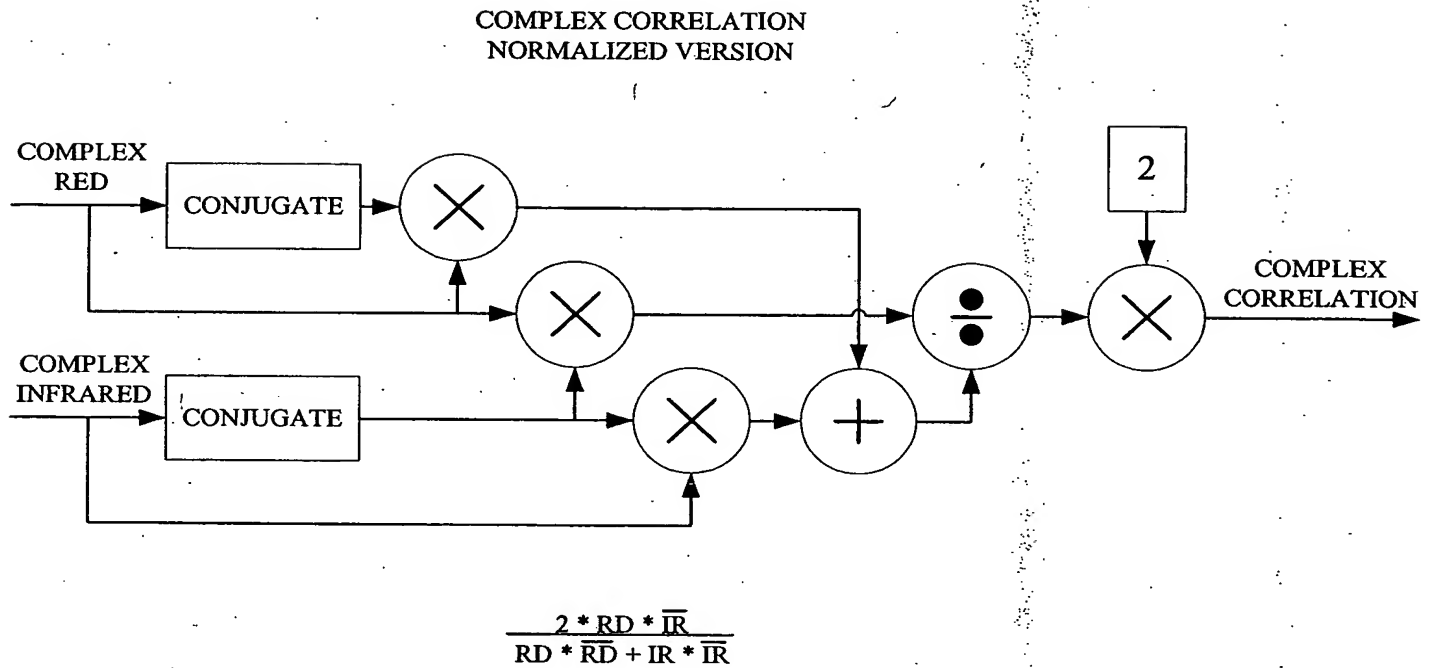


Figure 15. Block diagram to generate complex correlations

SYSTEMS AND METHODS FOR DETERMINING BLOOD  
OXYGEN SATURATION VALUES USING COMPLEX NUMBER  
ENCODING

Mohamed K. Diab

Appl. No.: Unknown Atty Docket: MLABS.021A  
13 / 24

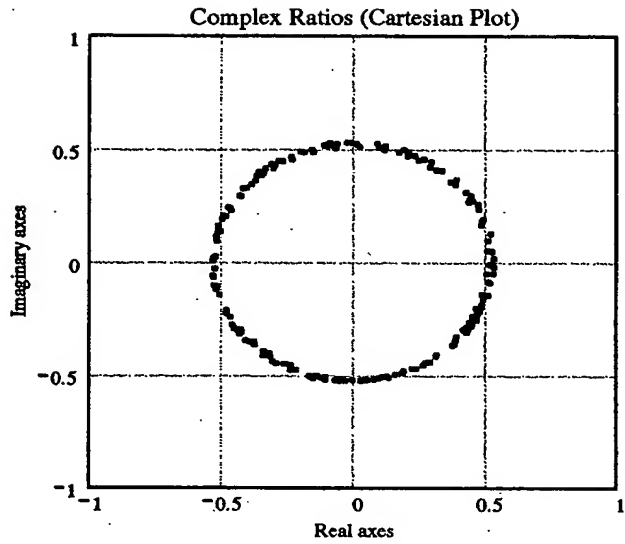


Figure 16. Complex ratios, steady saturation, for type B signals

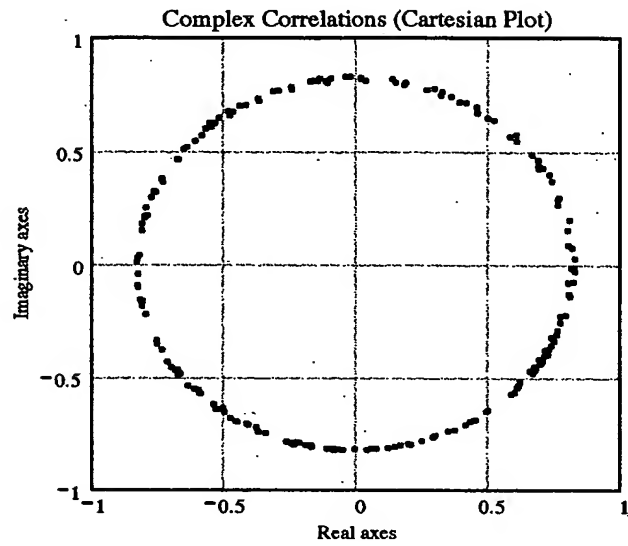


Figure 17. Complex correlations, steady saturation, for type B signals

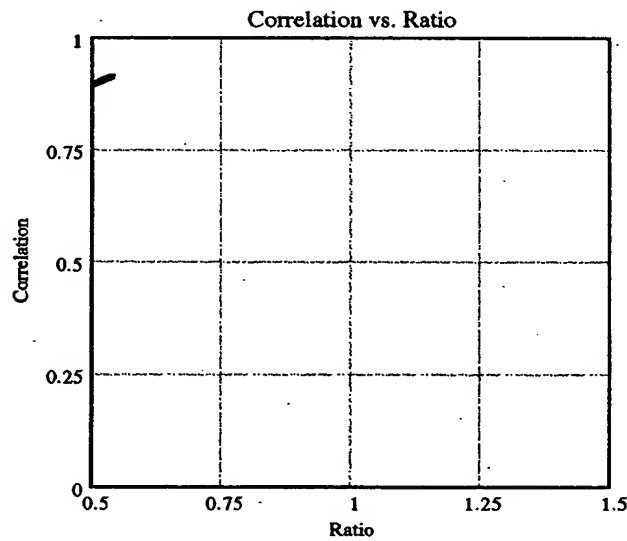


Figure 18. Square root of the magnitude of the complex correlation vs. ratio.

SYSTEMS AND METHODS FOR DETERMINING BLOOD  
OXYGEN SATURATION VALUES USING COMPLEX NUMBER  
ENCODING

Mohamed K. Diab

Appl. No.: Unknown Atty Docket: MLABS.021A  
14 / 24

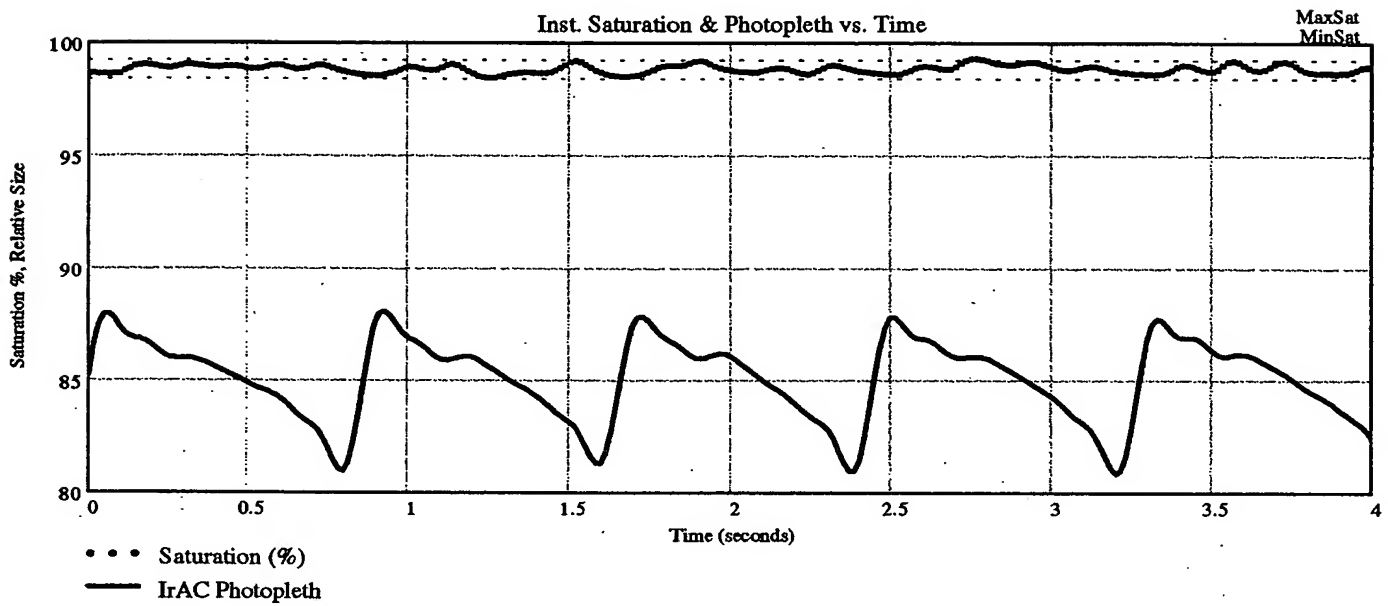


Fig. 19 Instantaneous saturation vs. time and corresponding Infrared photopleth

SYSTEMS AND METHODS FOR DETERMINING BLOOD  
OXYGEN SATURATION VALUES USING COMPLEX NUMBER  
ENCODING

Mohamed K. Diab

Appl. No.: Unknown Atty Docket: MLABS.021A

15 / 24

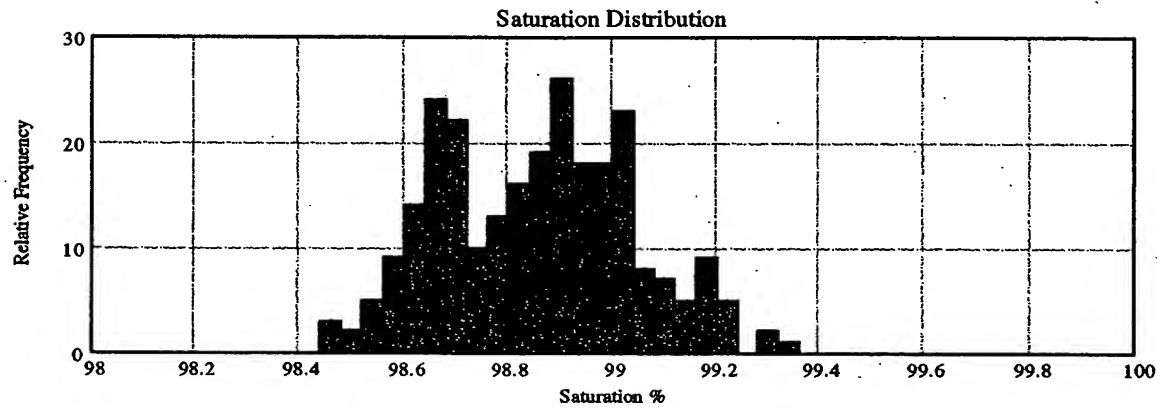


Fig. 20. Expanded view of the saturation distribution of the results of Figure 19. Note the bimodal shape of the distribution.

Standard Deviation

StdError = 0.18 %

Mean Satuartion Value

AverageSat = 98.9 %

Maximum Deviation from the mean

$\Delta$ Sat = 0.47 %

SYSTEMS AND METHODS FOR DETERMINING BLOOD  
OXYGEN SATURATION VALUES USING COMPLEX NUMBER  
ENCODING

Mohamed K. Diab

Appl. No.: Unknown Atty Docket: MLABS.021A  
16 / 24

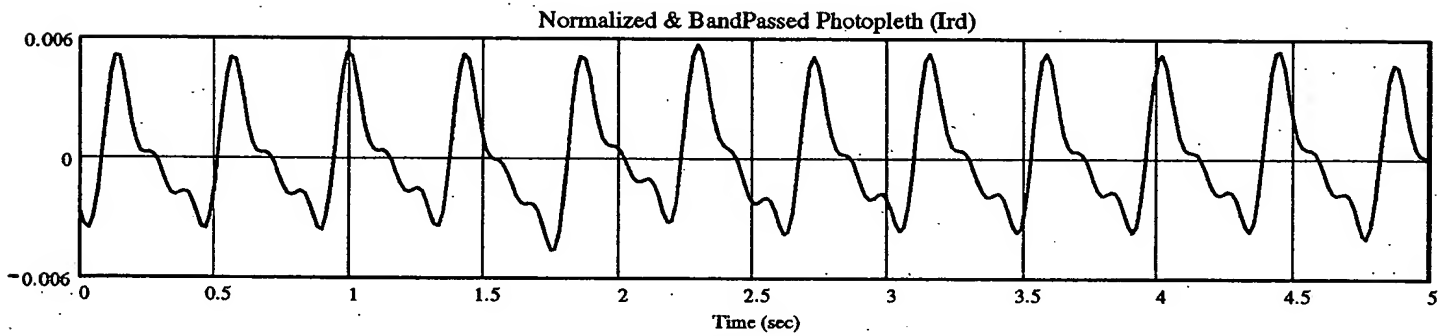


Figure 21. Infrared Photopleth

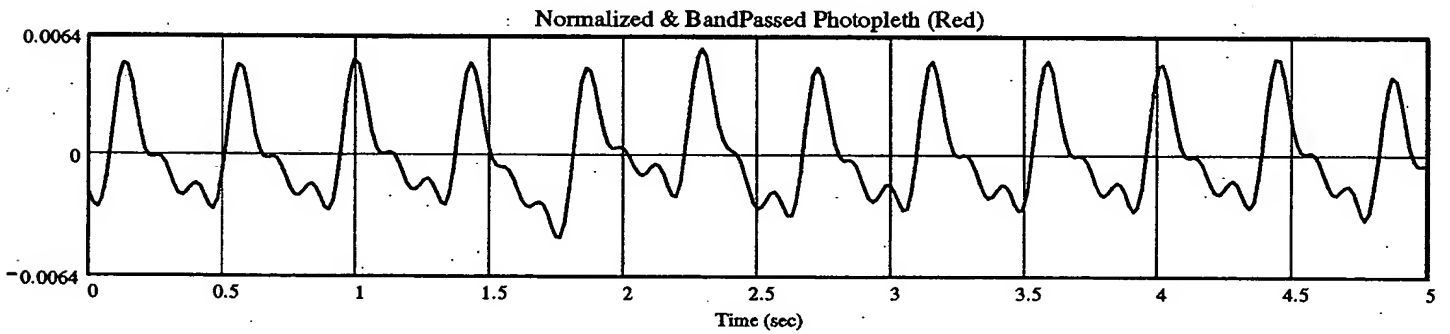


Figure 22. Red Photopleth



SYSTEMS AND METHODS FOR DETERMINING BLOOD  
OXYGEN SATURATION VALUES USING COMPLEX NUMBER  
ENCODING

Mohamed K. Diab

Appl. No.: Unknown Atty Docket: MLABS.021A  
17 / 24

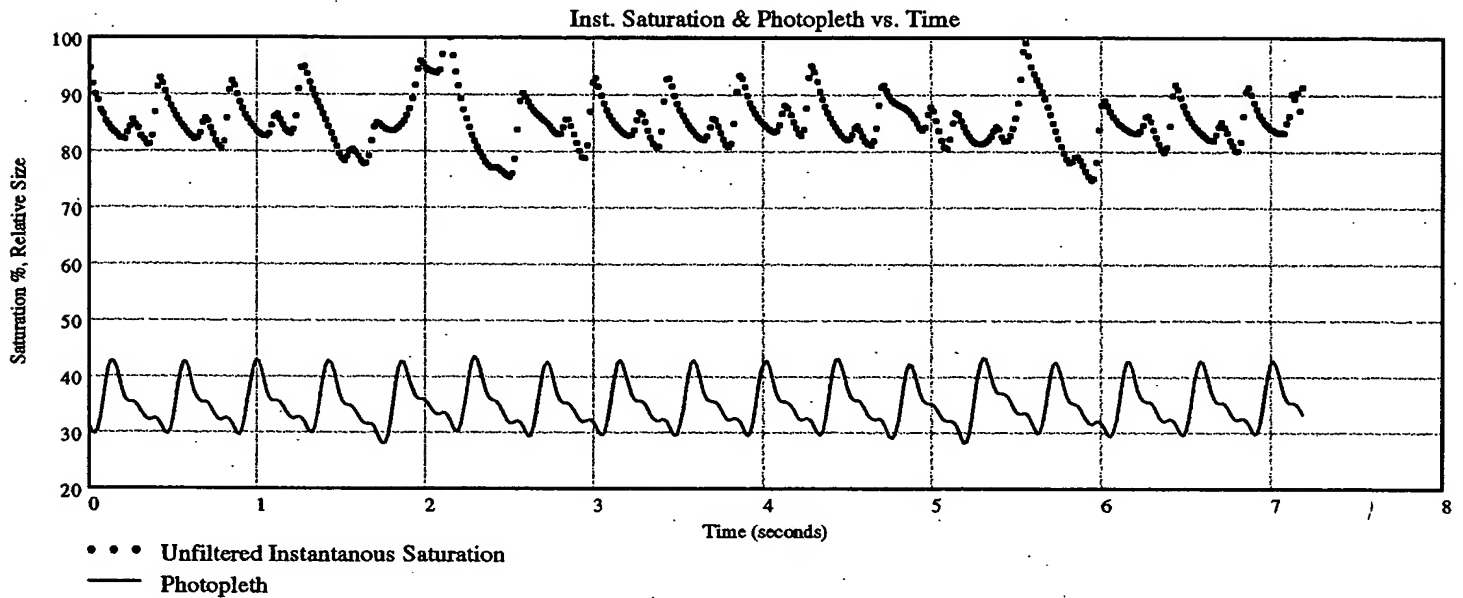


Figure 23. Instantaneous saturation with venous pulsation and photopleth vs.time

SYSTEMS AND METHODS FOR DETERMINING BLOOD  
OXYGEN SATURATION VALUES USING COMPLEX NUMBER  
ENCODING

Mohamed K. Diab

Appl. No.: Unknown      Atty Docket: MLABS.021A  
18 / 24

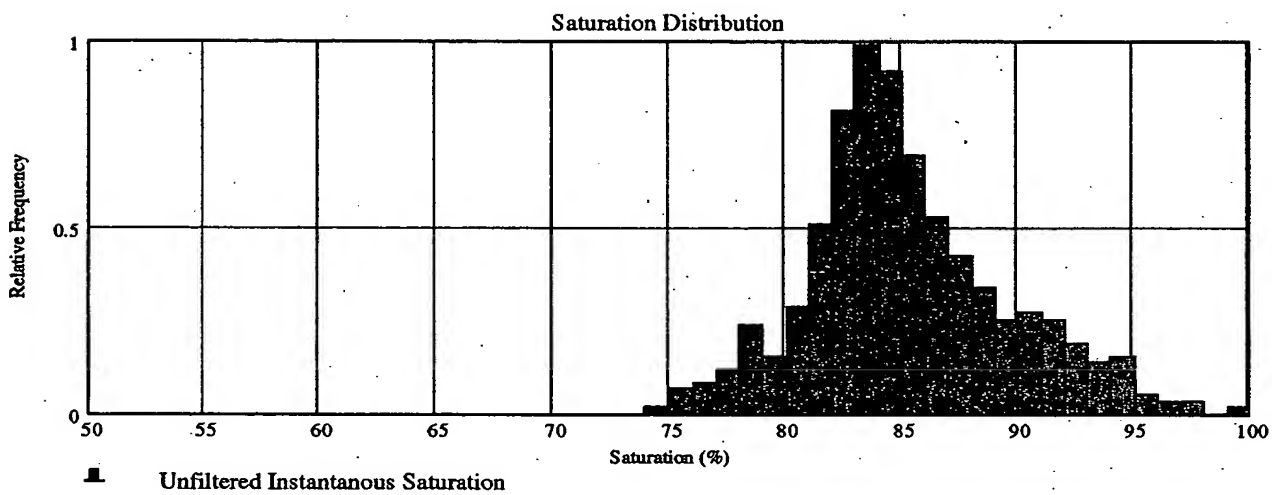


Fig. 24. Satuartion distribution of the data in Figure 23

Standard Deviation

StdError = 4.5 %

Mean Satuartion Value

AverageSat = 85.3 %

Maximum Deviation from the mean

$\Delta$ Sat = 25.13 %

Mode at 83.5%

SYSTEMS AND METHODS FOR DETERMINING BLOOD  
OXYGEN SATURATION VALUES USING COMPLEX NUMBER  
ENCODING

Mohamed K. Diab

Appl. No.: Unknown Atty Docket: MLABS.021A

19 / 24

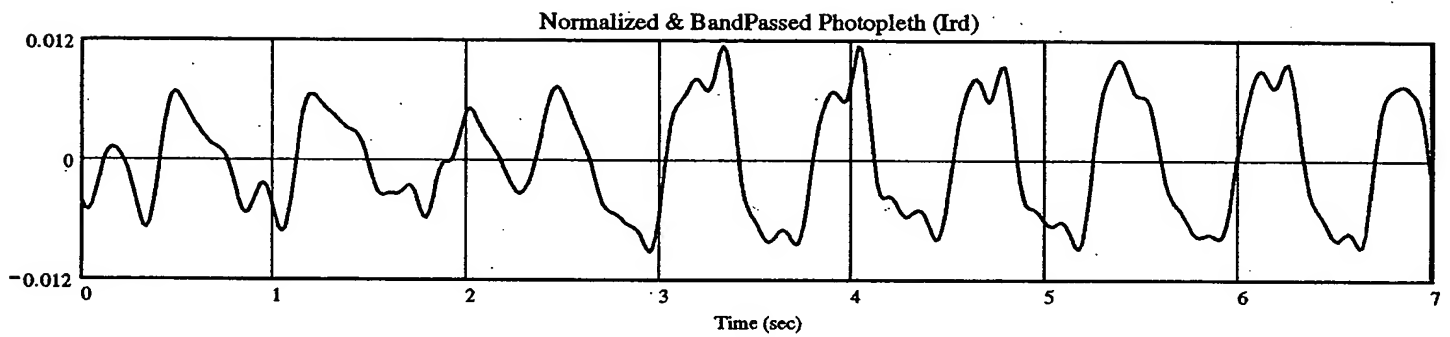


Fig. 25. Infrared Photopleth disturbed by motion artifacts

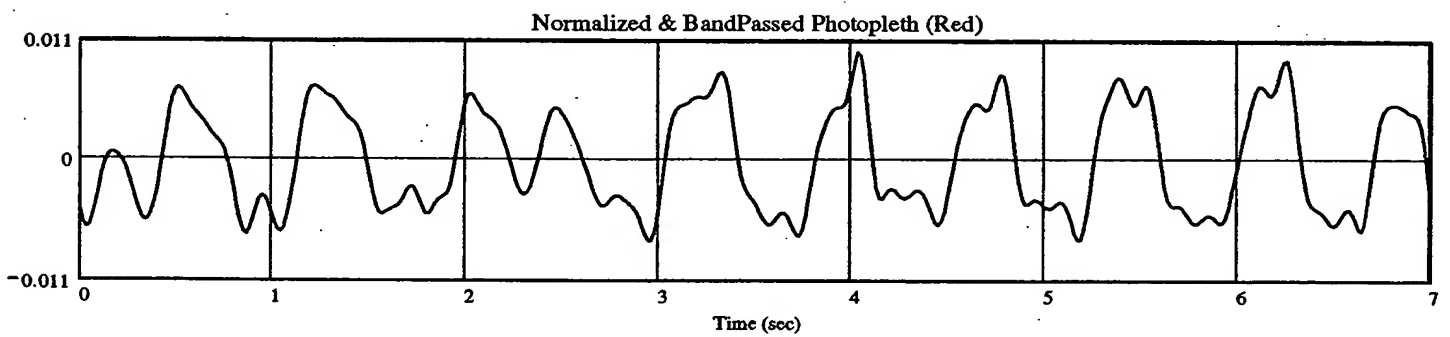


Fig. 26. Red Photopleth disturbed by motion artifacts

SYSTEMS AND METHODS FOR DETERMINING BLOOD  
OXYGEN SATURATION VALUES USING COMPLEX NUMBER  
ENCODING

Mohamed K. Diab

Appl. No.: Unknown    Atty Docket: MLABS.021A  
20 / 24

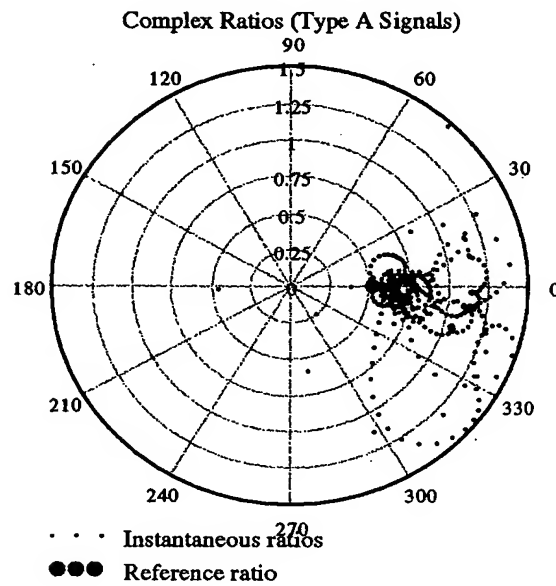


Fig 27. Polar plot of instantaneous ratios vs. phase angle

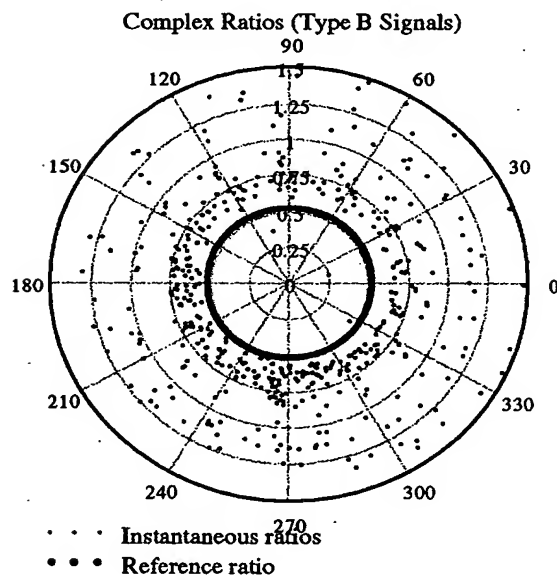


Fig 28. Polar plot of instantaneous ratios vs. phase angle

SYSTEMS AND METHODS FOR DETERMINING BLOOD  
OXYGEN SATURATION VALUES USING COMPLEX NUMBER  
ENCODING

Mohamed K. Diab

Appl. No.: Unknown Atty Docket: MLABS.021A  
21 / 24

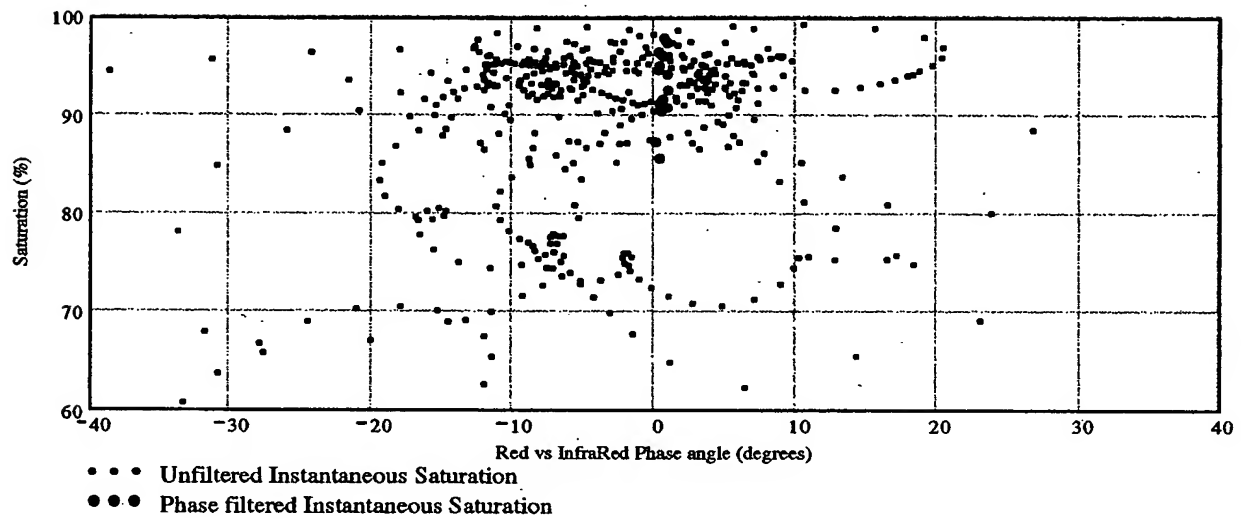


Fig. 29. Instantaneous saturation vs phase angle (degree)

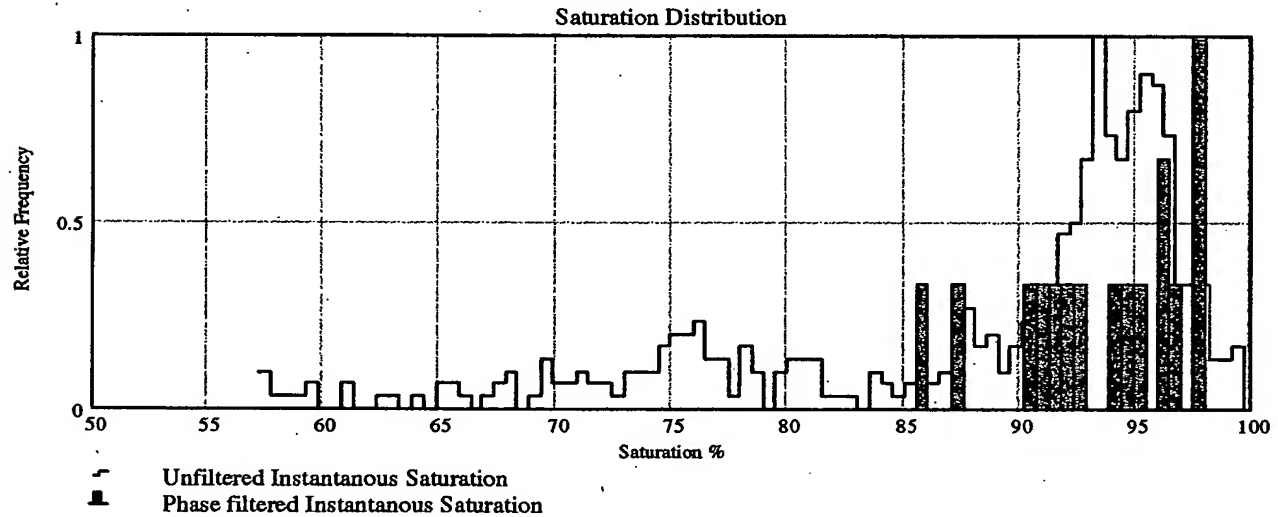


Fig. 30. Instantaneous saturation distribution

SYSTEMS AND METHODS FOR DETERMINING BLOOD  
OXYGEN SATURATION VALUES USING COMPLEX NUMBER  
ENCODING

Mohamed K. Diab

Appl. No.: Unknown Atty Docket: MLABS.021A

22 / 24

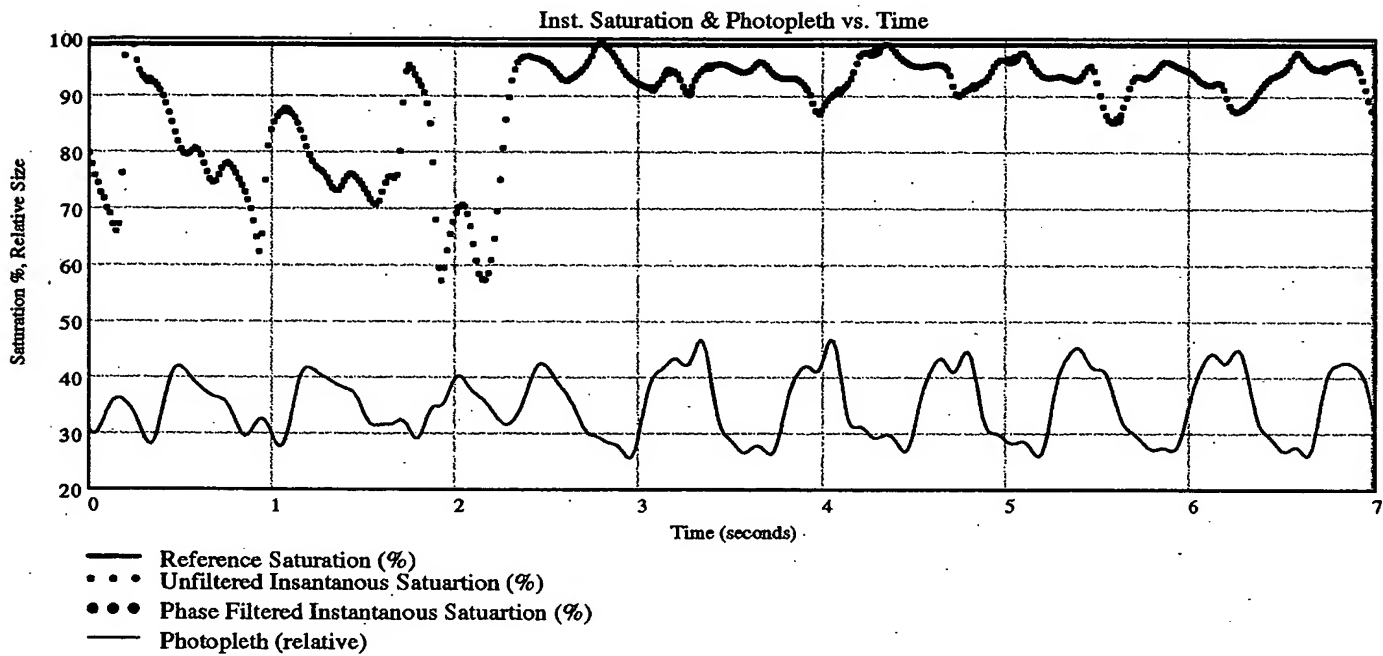


Figure 31. Instantaneous saturation with motion artifacts disturbance and photopleth vs. time

SYSTEMS AND METHODS FOR DETERMINING BLOOD  
OXYGEN SATURATION VALUES USING COMPLEX NUMBER  
ENCODING

Mohamed K. Diab

Appl. No.: Unknown Atty Docket: MLABS.021A

23 / 24

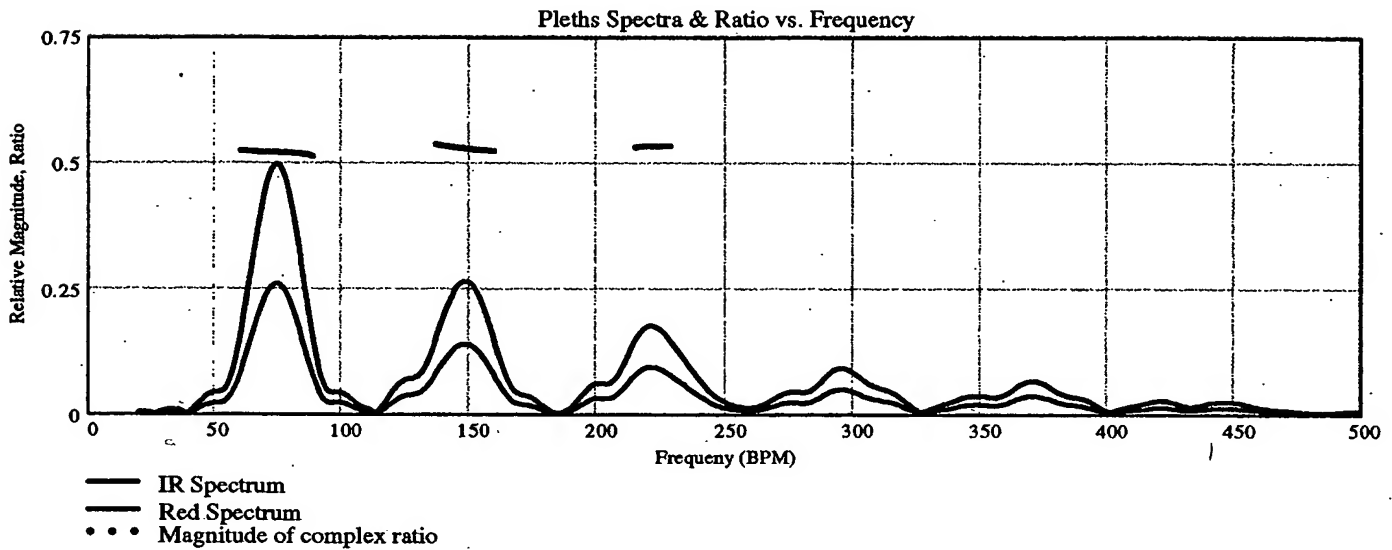


Figure 32. Magnitude of the frequency domain ratios for the photopleths shown in Figure 2.

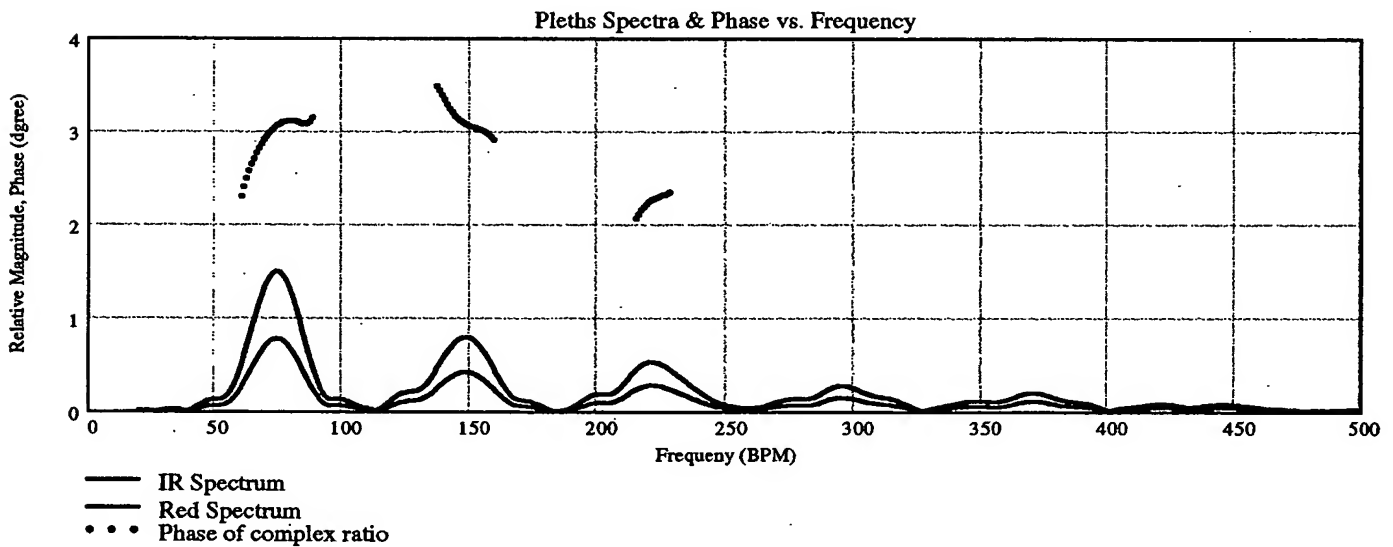


Figure 33. Phase (degrees) of the frequency domain ratios for the photopleths shown in Figure 2.

SYSTEMS AND METHODS FOR DETERMINING BLOOD  
OXYGEN SATURATION VALUES USING COMPLEX NUMBER  
ENCODING

Mohamed K. Diab

Appl. No.: Unknown Atty Docket: MLABS.021A  
24 / 24

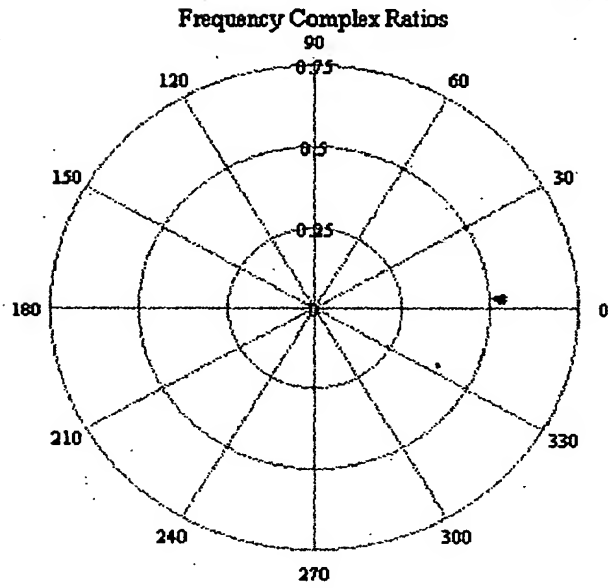


Figure 34: Polar plot of frequency complex ratios